Experimental Analysis of Impact Forces in Constrained Collisions According to ISO/TS 15066

Robin Jeanne Kirschner[1], Nico Mansfeld, Saeed Abdolshah and Sami Haddadin

Abstract— **For the user of a collaborative robot, it is important to select robot parameters and trajectories such that the task is fulfilled while ensuring human safety at the same time. In human robot interaction (HRI), constrained collisions can be particularly hazardous to the human and recently, collision test devices were developed that assess safety in such scenarios. In this paper, we propose the concept of a constrained collision force map (CCFM), which relates the robot impact velocity and the collision reaction method its parameterization to the peak collision force in a constrained collision scenario. The CCFM is a tool that will help practitioners to implement both safe and efficient HRI applications and to understand the robot's collision behavior. In this work, we derive the CCFM for three robots (UR10e, UR5e, and Franka Emika Panda) for varying contact thresholds, contact stiffnesses, and robot poses. Finally, we compare our results with the force estimation suggested by ISO/TS 15066:2016.**

I. INTRODUCTION

As the demand for HRI increases, it has become paramount to analyze the performance of different lightweight collaborative robots for their validation and for designing or selecting the most appropriate system for certain tasks. Well known performance metrics like pose repeatability, maximum reach, and payload should be extended by the robot's inherent safety characteristics as they are important for modern collaborative robots [1], [2], [3]. Such safety characteristics should consider human injury probability during contact [4], [6] and the robot's collision sensing and handling capabilities [5]. The current technical specification for safe HRI, ISO/TS 15066:2016 (ISO/TS) specifies that human pain onset (in particular in constrained contact settings) shall be avoided by limiting the contact force. The contact force in HRI depends on several factors, e.g., the robot speed, configuration, inertial, and surface properties, and the collision detection and reaction methods. There exist many methods to detect and identify collisions, which either rely on proprioceptive (motor current, joint torque) or exteroceptive robot measurements. An overview of common collision detection schemes is provided in [7].

For the robot user, it is difficult to predict or model contact forces in HRI. In this paper, we introduce the concept of constrained collision force maps (CCFM). A CCFM quantifies a robot's contact sensitivity in constrained contact scenarios depending on the collision detection parameters and the robot impact velocity. It is a practical tool that enables the user to understand the robot's impact behavior and to estimate the potential hazard during impacts. We experimentally derive the CCFM for three different robots, namely the Universal Robot's (UR) UR10e, UR5e, and the Franka Emika (FE) Panda, where we analyze the influence of collision thresholds, collision stiffnesses, and robot poses on the resulting peak impact force measured by a Pilz PRMS collision test device.

This paper is structured as follow. Section II gives an overview of collisions in physical HRI and possible benchmark tests. In Sec. III we introduce the idea of CCFMs. In Sec. IV-A and IV-B the experimental results of the considered robots are presented and force and torque thresholds are compared. Finally, Sec. V concludes the paper.

II. COLLISION BENCHMARKING IN HRI

To supply general performance benchmarks of industrial robots like repeatability and accuracy the standard ISO 9283:1998 was launched [8]. It defines a cube of reference positions applicable to every robot system. This cube is based on the robot minimum and maximum reach and shall be defined as typical operating workspace. ISO 9283:1998 provides guidelines how to apply this cube to obtain general performance metrics like pose repeatability. Benchmarks for motion planning are suggested in [9], which base on the user-experience. In [10] a collection of applied context dependent performance metrics for pHRI is presented. In the context of perception, authors mention applying metrics based on the signal detection and classification accuracy and describe those by success rate of recognition. Recently, collaborative robots task performance measurement is discussed and a standardized approach is introduced [11].

Obviously, also evaluating collision handling schemes requires experimental observation [7]. For robot safety based on ISO/TS [1] testing devices for collision forces were used to test robots compliance to safety [5]. Nevertheless, still no standardized procedure to evaluate the performance of collision reaction schemes especially according to their qualification on real systems is known to the authors. Therefore, we propose to use the existing devices for safety evaluation of collisions in HRI to generate a benchmark.

III. CCFM FOR BENCHMARKING CONSTRAINED COLLISIONS

A. Collision test device

The technical specification ISO/TS 15066:2016 [1] introduces a model of the human body, which covers 21 body regions. For each body region, a contact stiffness and a pain tolerance is provided. The hand thresholds of the body model are exemplary depicted in Fig. 1. These thresholds were derived in constrained contact situations, where the human body part was attached to a rigid surface for repeatable

[1]Authors are with Institute for Robotics and System Intelligence, Munich School of Robotics and Machine Intelligence, Technical University of Munich, 80797 Munich, Germany robin-jeanne.kirschner@tum.de

measurements [12]. We use the collision pressure measuring kit PRMS by company Pilz, to obtain forces curves and peak impact forces. It consists of a one-dimensional load cell, a spring, and a rubber cover. Multiple springs and three covers are available to adapt the stiffness according to the stiffness of the considered human body part.

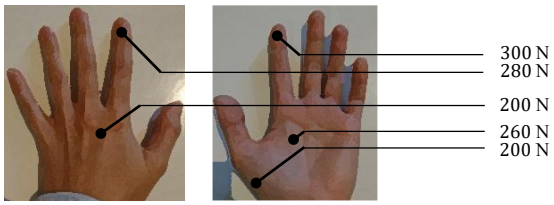

Fig. 1. Force thresholds for quasistatic contact on the dominant hand for HRI regarding to the bodymodel in ISO/TS [1].

B. Experimental design for deriving CCFMs

Using the PRMS force measurement set we investigate for the CCFMs by observing collision forces occurring during collisions using the most sensitive robot settings for UR10e, UR5e and FE Panda. As the human hand occurs to be the body part, which is most likely to be involved in a constrained collision we initially focus our assessment on a human hand model. We use a spring with constant $c = 75\,\mathrm{N/mm}$ and a cover with $70\,\mathrm{ShA}$ for the human hand. The force threshold for transient contact given by the PRMS device in accordance to ISO/TS is $280\,\mathrm{N}$ and the quasi-static threshold is $120\,\mathrm{N}$. To define a comparable position for the collision we defined each robot's reference cube according to DIN EN ISO 9283 [8]. The PRMS device is mounted to the table as shown in Fig.2 and we use a Cartesian motion generator to collide with the PRMS device at a desired speed. Due to the maximum permissible collision force of $500\,\mathrm{N}$ for the PRMS device we start with $0.05\,\mathrm{m/s}$ and stop at $0.61\,\mathrm{m/s}$.

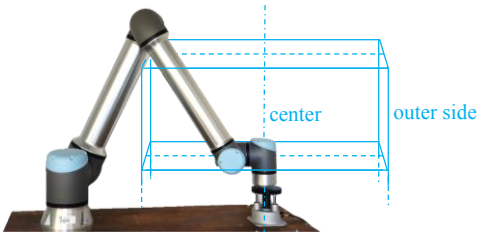

Fig. 2. Experimental setup based on the reference cube and the PRMS collision test device for evaluating the constrained contact sensitivity of a robot demonstrated by a UR10e robot.

Using the generated data, we establish the CCFMs, which depict the peak force occurring at a collision depending on the collision threshold and contact velocity. This peak impact force is inherently related to the reactiveness of the robot and may exceed the defined collision thresholds. As most robots are capable to provide collision force thresholds of $100\,\mathrm{N}$, we designed the map to consider force thresholds up to $100\,\mathrm{N}$ maximum. Nevertheless, some tactile robots provide also torque limitation, which may lead to more sensitive reaction schemes. We, therefore, investigate if the torque limitation decreases the peak collision forces compared to the force limitation. Due to the mass-force relation we include an analysis of different positions for collision and additionally observe the effect of low contact stiffness on the peak impact force.

C. The influence of collision reaction

The robot's collision reaction can contribute to the impulse transferred at a collision. Following, we therefore look at the implemented collision reaction of UR and FE Panda. At collision, the UR robots show a retracting motion depicted in Fig. 3. During the collision, the motion of the UR is reversed and the constrained contact released.

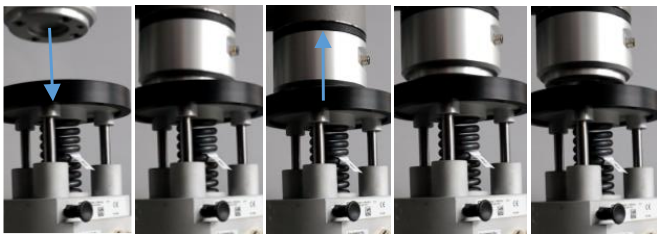

Fig. 3. Retracting motion of UR robots at collision.

The FE Panda's collision reaction relies on its compliance. Instead of triggering a backwards motion, it stops and due to its low joint stiffness the force on the contact is released as shown in Fig. 4.

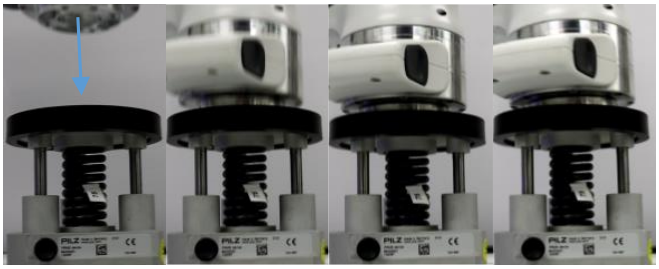

Fig. 4. Braking motion of FE Panda at collision.

IV. Peak Impact Forces as Measure of CCFMs

A. UR robots

The UR robots both enable to set the safety thresholds for collision to $F_{\max} = 100\,\mathrm{N}$. Therefore, we observe the peak forces occurring during the constrained collision using this setting. Fig. 5 and 6 depict the force curves derived with velocities between $0.05\,\mathrm{m/s}$ and $0.54\,\mathrm{m/s}$. For the UR10e and UR5e of collisions notice that according to ISO/TS 15066:2016 the thresholds for transient contact with a human hand are fulfilled below $0.26\,\mathrm{m/s}$. Surprisingly, the results for UR5e with velocities above $0.4\,\mathrm{m/s}$ show a second increase in force at around $400\,\mathrm{ms}$. We assume this is a result of the collision reaction mechanism.

To obtain the CCFMs in Fig. 7 and Fig. 8 we map the recorded maximum peak forces to the collision constraint setting and the applied collision velocity.

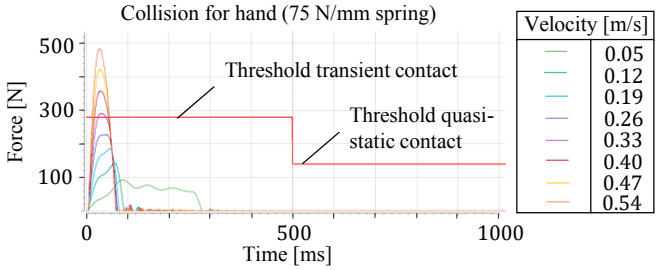

Fig. 5. Force over time measured with the PRMS device of the UR10e.

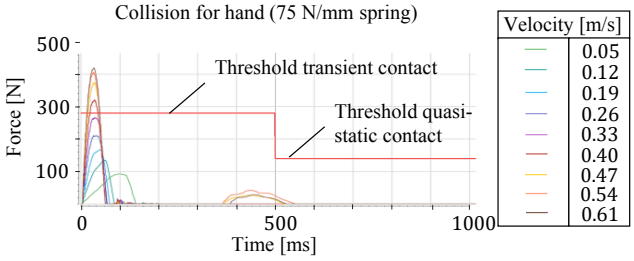

Fig. 6. Force over time measured with the PRMS device of the UR5e.

B. *Franka Emika Panda*

Similar experiments are conducted with the FE Panda. The force curve for the threshold 100 N is depicted by Fig. 10. Besides the threshold 100 N FE Panda allows to set lower force thresholds from which we obtain the following CCFM in Fig. 9.

For comparison of applying joint torque thresholds instead of end effector force thresholds, we investigate the most sensitive torque threshold, which is applicable using our motion generator (Cartesian fourth order) and derive the peak impact forces.

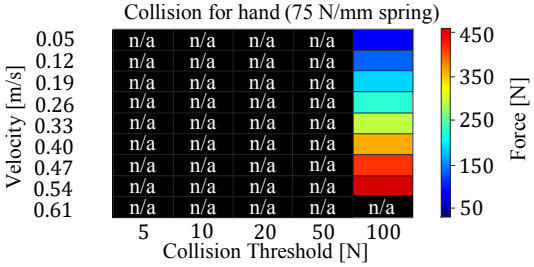

Fig. 7. CCFM of UR10e with maximum contact sensitivity settings 100 N.

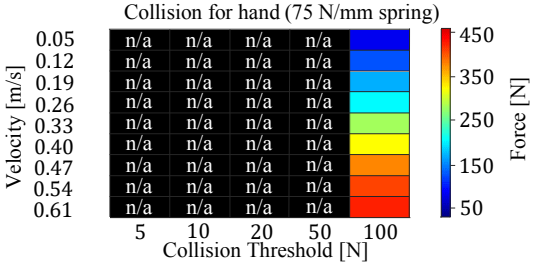

Fig. 8. CCFM of UR5e with maximum contact sensitivity setting 100 N.

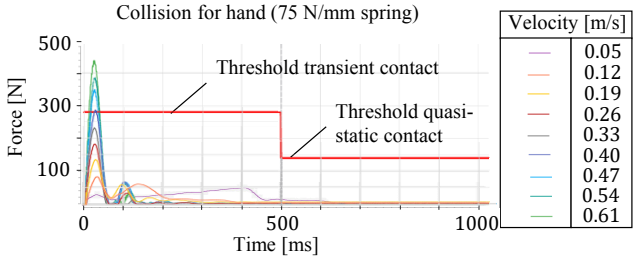

Fig. 9. Force over time measured with the PRMS device of the FE Panda.

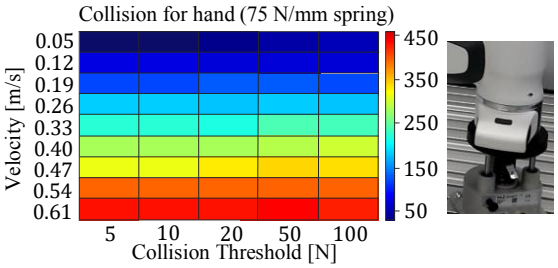

Fig. 10. CCFM of FE Panda with various contact sensitivity settings.

C. *Effect of collision thresholds on peak impact force*

With these experiments, we find that setting the collision thresholds hardly influences the maximum force measured by the PRMS device. It can be observed that using thresholds below $F_{\max} = 20\,\mathrm{N}$ decreases the peak impact force in contacts with low velocities like $0.05\,\mathrm{m/s}$. As already reported in [13], the application of collision reaction schemes appears to be unable to mitigate the occurring peak impact forces. As we can see from Fig. 9 and 11 the time, in which the impact force builds up within the first approx. $5\,\mathrm{ms}$ resulting in an even shorter time frame for collision detection and reaction. We conclude that with the PRMS device using the $75\,\mathrm{N/mm}$ spring an almost rigid contact occurs leaving few time for improving the collision force by collision reaction and detection. UR5e and FE Panda only differ slightly considering the occurring peak forces while the UR10e, which has a higher mass causes significantly higher forces, suggesting that differing results between FE Panda and both UR robots are based on the robots' masses. Therefore, major changes of the effective mass are expected considering different points inside the robot workspace.

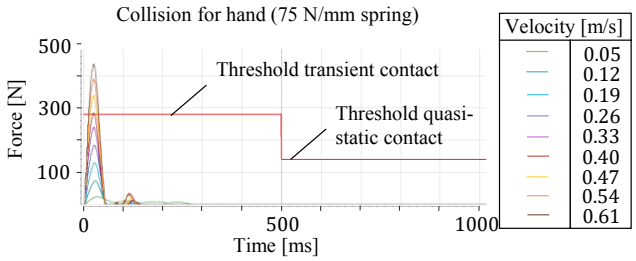

Fig. 11. Forces curves for collisions with threshold $[2.5, 2.5, 2.0, 2.0, 1.5, 1.5, 1.0]$ Nm measured with the PRMS device of the FE Panda

D. Effect of contact stiffness on peak impact force

The influence of the spring stiffness and the material stiffness on the robots collision performance becomes visible, when equipping the CCFM for a collision with an abdominal muscle in comparison to the CCFMs derived for the human hand in Section IV-B. The model of the abdominal muscle consists of a spring $c = 10\,\mathrm{N/mm}$ and a covering material with $10\,\mathrm{ShA}$, shown in Fig. 12. The more flexible contact seemingly decelerates the increase of the force at the collision and enables the robots sensing systems and controller to react sooner. This leads to a visible effect of using lower collision thresholds on the peak forces occurring during the collision. At velocity $0.05\,\mathrm{m/s}$ and $5\,\mathrm{N}$ and $10\,\mathrm{N}$ the peak impact force is not detected by the sensor integrated to the PRMS device.

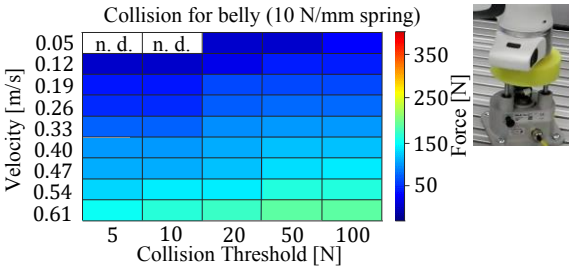

Fig. 12. CCFM for FE Panda at collisions with the abdominal muscle with spring constant $c = 10\,\mathrm{N/mm}$ and covering material with $10\,\mathrm{ShA}$.

E. Effect of robot pose on peak impact force

Next, we consider two different positions for the collision; at the centre of the reference cube and $-5\,\mathrm{cm}$ from its outer side. We obtain lower peak forces at the outer edge, which can be explained by the orientation of the robot's link 5 depicted in Fig. 13. At the first collision point it is almost vertical while at the second it is tilted about $45°$ to the ground. Therefore, less of its mass contributed to the occurring impact force. Generally, the results in Fig. 13 named center and outer side demonstrate that the effective mass and, therefore, the pose of the robot influences the peak impact force.

F. Comparison to force estimation using ISO/TS 15066

Based on Sec. IV-E we evaluated the difference in force predicted by the collision model in ISO/TS 15066:2016 and our measurements. The maximum contact force according to the model is

$$F_{\mathrm{col}} = v_{rel}\sqrt{\mu k}\,, \tag{1}$$

where k is the contact stiffness of the body part (human hand ($k = 75\,\mathrm{N/mm}$) in our experiment), v_{rel} the relative velocity, and μ the effective mass between human and robot [1]

$$\mu = \left(\frac{1}{m_{\mathrm{r}}} + \frac{1}{m_{\mathrm{h}}}\right)^{-1}. \tag{2}$$

The human mass is m_{h} (for the human hand $m_{\mathrm{h}} = 0.6\,\mathrm{kg}$) and the robot mass is

$$m_{\mathrm{r}} = M/2 + m_{\mathrm{L}}\,, \tag{3}$$

where the total mass of all moving links is denoted by M, and the load m_{L} [1]. For each considered velocity we calculate the estimated force based on ISO/TS 15066:2016 and compare these values to our previous results in Fig. 13. For each impact we observe a significant underestimation in contact force.

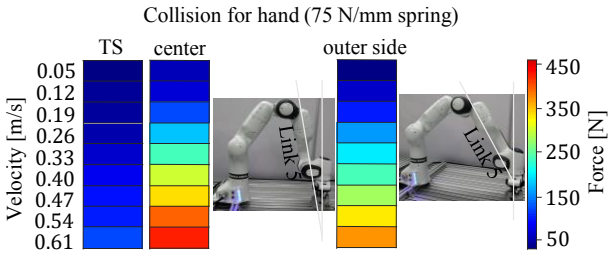

Fig. 13. CCFM for FE Panda with 100N threshold at outer side and centre of the reference cube compared to the results for estimating the force by ISO/TS 15066 (TS).

V. Discussion and Conclusion

In this paper, we introduced constrained collision force maps (CCFMs) as a benchmark for evaluating the collision behavior of collaborative robots in constrained collision scenarios. The CCFM is a practical tool that helps the user to implement safe robot applications and understand the collision behavior of his/her robot. We experimentally derived the CCFM for the UR10e, UR5e, and the Franka Emika Panda using different collision velocities and robot collision detection thresholds. Additionally, we investigated the difference in contact sensitivity between torque- and force-based collision thresholds. In terms of the absolute value of the collision thresholds, no noticeable influence on resulting peak contact forces was observed when using a high contact stiffness. Considering lower contact stiffness, however, the collision detection thresholds do influence the peak collision force. The varying peak impact forces among the three robots observed for high contact stiffness can most likely be explained by the significantly different inertial properties. Lastly, a comparison between our measurements and the collision force model in ISO/TS 15066:2016 showed large differences, which implies that the ISO/TS model is not well suited for estimating collision forces. The derivation of the CCFM for further robot workspace locations and the analysis of additional robots like the KUKA iiwa or the Techman TM5 is subject to future work.

Acknowledgment

The authors would like to thank Joao Jantalia for helping with conducting the experiments. We gratefully acknowledge the funding of the Lighthouse Initiative Geriatronics by StMWi Bayern (Project X, grant no. 5140951) and LongLeif GaPa gGmbH (Project Y, grant no. 5140953), the European Union's Horizon 2020 research and innovation program as part of the project ILIAD under grant no. 732737 and the support by the European Union's Horizon 2020 research and innovation program as part of the project I.AM. under grant no. 871899. Please note that S. Haddadin has a potential conflict of interest as shareholder of Franka Emika GmbH.

REFERENCES

[1] ISO/TS 15066:2017, *Robots and robotic devices - Collaborative robots*, Beuth-Verlag, Berlin.

[2] V. Bhanoday, B Matthias, A. Ahmad. "A design metric for safety assessment of industrial robot design suitable for power-and force-limited collaborative operation." International journal of intelligent robotics and applications 2.2 (2018): 226-234.

[3] D. Kirschner, A. Schlotzhauer, M. Brandstötter, M. Hofbaur, "Validation of Relevant Parameters of Sensitive Manipulators for Human-Robot Collaboration," in Advances in Service and Industrial Robotics, RAAD 2017, Mechanisms and Machine Science, 2018, vol 49. Springer, Cham.

[4] S. Haddadin, S. Haddadin, A. Khoury, T. Rokahr, S. Parusel, R. Burgkart, A. Albu-Schäffer, "On making robots understand safety: Embedding injury knowledge into control", *The International Journal of Robotics Research*, vol. 31, 13th ed, 2012, pp. 1578?1602.

[5] A. Schlotzhauer, L. Kaiser, J. Wachter, M. Brandstötter and M. Hofbaur, "On the trustability of the safety measures of collaborative robots: 2D Collision-force-map of a sensitive manipulator for safe HRC," 2019 IEEE 15th International Conference on Automation Science and Engineering (CASE), Vancouver, BC, Canada, 2019, pp. 1676-1683.

[6] N. Mansfeld, M. Hamad, M. Becker, A. G. Marin and S. Haddadin, "Safety Map: A Unified Representation for Biomechanics Impact Data and Robot Instantaneous Dynamic Properties," in IEEE Robotics and Automation Letters, vol. 3, no. 3, pp. 1880-1887, July 2018.

[7] S. Haddadin, A. De Luca and A. Albu-Schäffer, "Robot Collisions: A Survey on Detection, Isolation, and Identification," in IEEE Transactions on Robotics, vol. 33, no. 6, pp. 1292-1312, Dec. 2017.

[8] ISO 9283:1998, *Manipulating industrial robots - Performance criteria and related test methods*, Beuth Verlag, Berlin.

[9] B. Cohen, I. A. Şucan and S. Chitta, "A generic infrastructure for benchmarking motion planners," 2012 IEEE/RSJ International Conference on Intelligent Robots and Systems, Vilamoura, 2012, pp. 589-595.

[10] A. Steinfeld, et al. "Common metrics for human-robot interaction," 2006 1st ACM SIGCHI/SIGART conference on Human-robot interaction (HRI '06), New York, NY, USA, 2006. 33-40.

[11] K. Kimble, K. Van Wyk, J. Falco, E. Messina, Y. Sun, M. Shibata, W. Uemura, and Y. Yokokohji, Benchmarking Protocols for Evaluating Small Parts Robotic Assembly Systems, IEEE Robotics and Automation Letters, vol. 5, no. 2, pp. 883-889, 2020.

[12] R. Behrens, "Biomechanische Grenzwerte für die sichere Mensch-Roboter-Kollaboration." Springer Vieweg, in Springer Fachmedien Wiesbaden GmbH, 2019.

[13] S. Haddadin, A. Albu-Schffer, and G. Hirzinger. "Dummy crash-tests for the evaluation of rigid human-robot impacts." International Workshop on Technical Challenges for dependable robots in Human Environments. 2007.